Optically and Thermally Induced Electron Transfer Pathways in Hexakis[4-(*N*,*N*-diarylamino)phenyl]benzene Derivatives

Christoph Lambert* and Gilbert Nöll[a]

Dedicated to Professor Manfred Christl on the occasion of his 60th birthday

Abstract: The optically and thermally induced electron transfer pathways of highly symmetrical (D_3) hexaarylbenzene systems with six triarylamine redox sites have been investigated. Owing to slightly different local redox potentials, the radical trication could be selectively generated by electrochemical methods. This trication shows a strong intervalence charge-transfer band in the near infrared (NIR) that was measured by spectroelectrochemistry and analysed using multi-dimensional Mulliken–Hush theory. Quantum chemical AM1 CI calculations indicate that there is no optically induced concerted three-electron transfer that transforms the ground state into a state in which all three positively charged triarylamine moieties change place with their neutral neighbours. The potential energy surface of the ground state was constructed by using quadratic potentials. From this potential surface it is apparent that there is also no thermally allowed concerted three-electron transfer pathway. Instead, three consecutive one-electron transfer steps are necessary for this process.

Keywords: cyclic voltammetry · electron transfer · mixed-valent compounds · spectroelectrochemistry · triarylamines

Introduction

Herein we investigate the optically induced electron transfer pathways that proceed in hexaarylbenzene derivatives with six triarylamine redox moieties.

Electron transfer (ET) plays a fundamental role in chemistry[1] and biology.[2] Innumerable studies have been devoted to intramolecular ET processes in biological, biomimetic and completely artificial systems. The most basic aspects of intramolecular ET were studied in so-called mixed-valence complexes in which two metal redox centres with different oxidation states are connected by a bridge which mediates the ET by mixing donor and acceptor wave functions.[3–5] In contrast to these well-known inorganic mixed-valence species, much less is known about purely organic representatives in which two organic redox-active moieties, such as hydrazines, triarylamines or quinones, are bridged by a saturated or unsaturated spacer.[6–22] This spacer mediates the ET by a super-exchange mechanism where the electron is never located vibronically at the bridge.[23]

The inorganic and organic mixed-valence species are characterised by usually weak and broad absorption bands in the NIR that are associated with an optically induced ET (intervalence charge transfer, IV-CT). Analysis of this IV-CT band within the framework of the Mulliken–Hush theory[24–28] leads to an electronic coupling element which describes the coupling of two usually degenerate diabatic states (φ_a and φ_b) in which the electron is localised at one redox site or the other, respectively. Within this theoretical approach, two diabatic states are coupled in a 2 × 2 secular determinant to give two adiabatic states ψ_g and ψ_e. Excitation from one minimum of the lower potential energy surface (ψ_g) to the excited CT state (ψ_e) gives rise to the observed absorption in the NIR. From the transition moment (μ_{eg}) for this excitation, the IV-CT energy ($\tilde{\nu}_{max}$) and the dipole moment difference between both diabatic states ($\Delta\mu_{ab}$), one can calculate the electronic coupling by using Equation (1).[29]

$$V = \frac{\mu_{eg}\tilde{\nu}_{max}}{\Delta\mu_{ab}} \tag{1}$$

The transition moment (μ_{eg}) can be obtained from the integrated absorption band by using Equation (2). The dipole

$$\mu_{eg} = 0.09584\sqrt{\frac{\int \varepsilon(\tilde{\nu})\mathrm{d}\tilde{\nu}}{\tilde{\nu}_{max}}} \tag{2}$$

moment difference of the diabatic states ($\Delta\mu_{ab}$) can either be replaced by er, where r is the effective ET distance estimated by the geometric distance of the redox centres (this is a good approximation in the weak coupling regime only),[20]

---

[a] Prof. Dr. C. Lambert, Dr. G. Nöll
Institut für Organische Chemie, Julius-Maximilians-Universität Würzburg, Am Hubland, 97074 Würzburg (Germany)
Fax: (+49) 931-888-4606
E-mail: lambert@chemie.uni-wuerzburg.de

or can be calculated by purely adiabatic quantities by using Equation (3) in which $\Delta\mu_{gg}$ is the difference of adiabatic dipole moment of the two minima and μ_{eg} is the transition moment (generalised Mulliken–Hush theory).[26, 28]

$$\Delta\mu_{ab} = \sqrt{(\Delta\mu_{gg})^2 + 4(\mu_{eg})^2} \quad (3)$$

The theoretical analysis mentioned above is rather straightforward in simple one-dimensional ET systems. However, the situation is much more complex if three or even more redox sites are involved in a single mixed-valence species. Then, the question arises whether two or more electrons can be transferred in a concerted or stepwise manner. Very few studies are available that report theoretical[30–34] or experimental[21, 35–39] studies on multi-dimensional ET systems, but these do not address the above-mentioned question. Quite recently,[40] we have shown that in the case of the diradical trication of the pseudotetrahedral tetrakis{4-[*N,N*-di(4-methoxyphenyl)amino]phenyl}phosphonium ion ($\mathbf{1}^+$) the electron transfer is stepwise both thermally and optically induced. Herein, we apply a similar methodology to elucidate the electron transfer pathways in symmetrical and asymmetrical hexaarylbenzene derivatives with six triarylamine redox moieties. These systems may be regarded as small dendrimeric units. Dendrimers based on hexaarylbenzene moieties have recently gained much interest because of their materials' properties.[41–43] In addition, dendrimers comprising triarylamine moieties[44–57] were studied for their hole-transport properties and used as components in organic light-emitting devices for example.

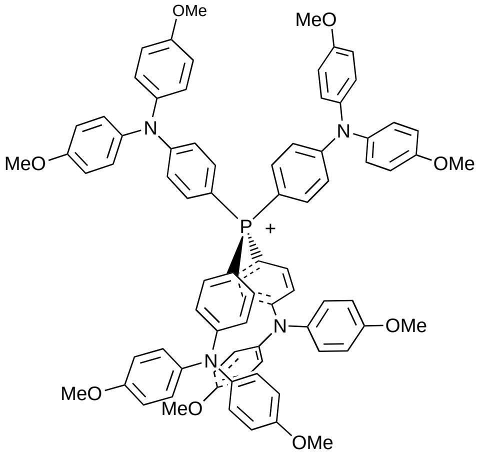

$\mathbf{1}^+$

Results and Discussion

Synthesis: The cobalt-catalysed trimerisation of tolanes is a well-known method for the synthesis of hexaarylbenzenes.[58] In this way, highly functionalised dyes can easily be built up from substituted tolanes. We started from bis{4-[*N,N*-di-(4-methoxyphenyl)amino]phenyl}acetylene (**2**) which trimerised in the presence of $[Co_2(CO)_8]$ catalyst to afford the symmetrical hexakis{4-[*N,N*-di(4-methoxyphenyl)amino]phenyl}benzene (**3**) in 60% yield (Scheme 1); properties of **3** were preliminarily reported elsewhere.[21] The *para* positions of the phenylamine groups were protected to guarantee reversible redox behaviour. However, this compound suffers from the disadvantage that the trication cannot be selectively generated because the six redox potentials are too close and, consequently, the comproportionation constants are too small. For this reason, we synthesised a tolane with two different triarylamine moieties: one in which the *para* positions are again protected by methoxy groups and the other triarylamine moiety in which the *para*-positions are protected by methyl groups (**4**). These different substituents lead to different local redox potentials of the two triarylamine units and to a non-degeneracy of the diabatic potentials, which now differ by ΔG^0. This ΔG^0 shift can be estimated by the shift of the IV-CT band energy of **2** versus **4** in CH_2Cl_2 which is 290 cm^{-1}.[59] $[Co_2(CO)_8]$-catalysed trimerisation of **4** gave two regioisomers **5** and **6** in 20% and 60% yield, respectively, which could be separated by flash chromatography (Scheme 2). The ratio of yields corresponds exactly to the statistical (1:3) formation of the 1,3,5 and 1,2,4 isomers. Therefore, the electronic influence of the MeO- and Me-substituents is confined to the triarylamine moieties and these

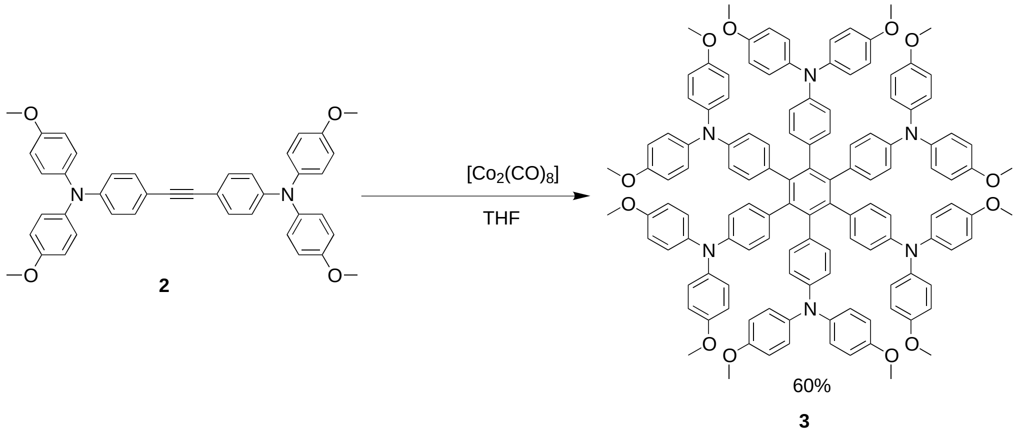

Scheme 1. Synthesis of **3** by $[Co_2(CO)_8]$-induced trimerisation of **2**.

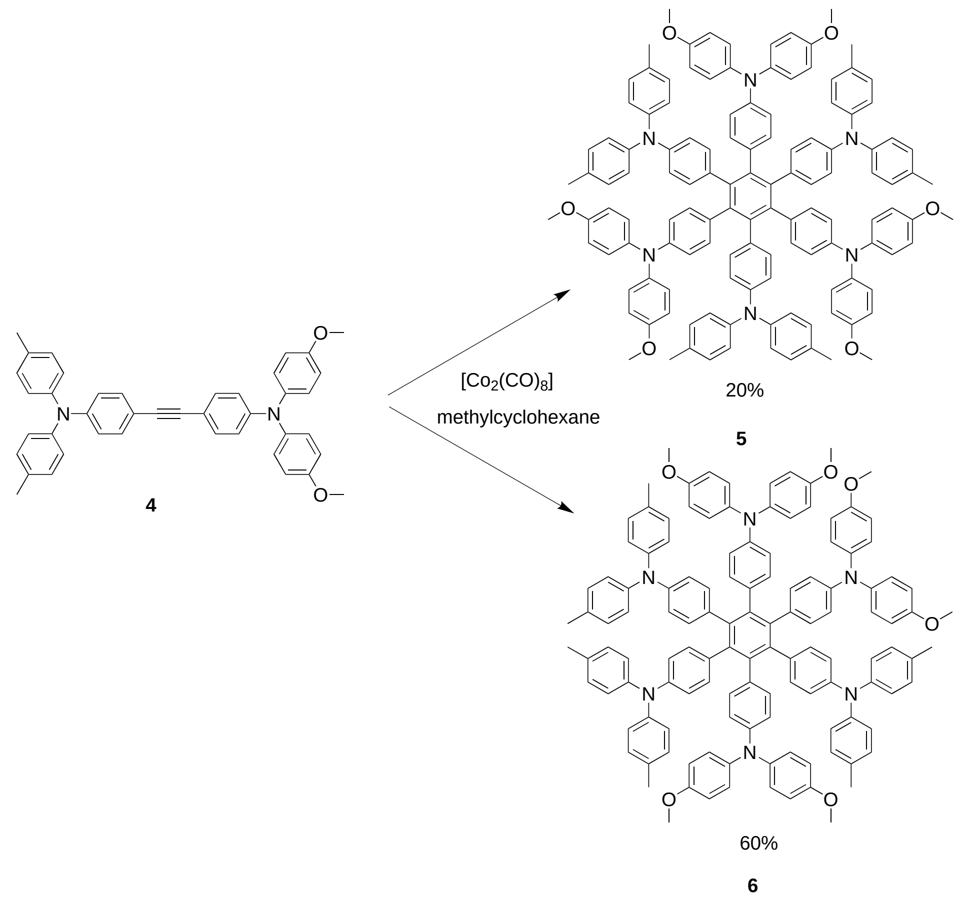

Scheme 2. Synthesis of **5** and **6** by $[Co_2(CO)_8]$-catalysed trimerisation of **4**.

substituents have no influence on the regiochemistry of the trimerisation with $[Co_2(CO)_8]$.

Electrochemistry: The redox potentials of trimers **3**, **5** and **6** were measured by cyclic voltammetry (CV) in CH_2Cl_2/0.1 M TBAH (see Figure 1). For trimer **3**, a reversible unresolved anodic wave was observed for the six consecutive redox processes. In stark contrast, **5** and **6** had two reversible waves corresponding to three one-electron redox processes close in potential. This splitting into two sets of three one-electron transfer processes is due to the potential tuning by the methyl and methoxy substituents. Digital fitting[60] of the cyclic voltammograms of **3**, **5** and **6** with the assumption of electrochemical and chemical reversibility gave the redox potentials of the six redox processes (see Table 1).

In **5** and **6** we assume that the first wave covers the oxidation steps of the three methoxy-substituted triarylamine moieties, and that the second wave covers the three oxidations steps of the methyl-substituted moieties. Interestingly, the redox potentials of **5** and **6** differ only slightly. This is surprising given the different positions of the methoxy-substituted triarylamines and indicates that the differences in electrostatic repulsion between the radical cation triarylamine moieties within the 1,3,5-substituted **5** and the 1,2,4-substituted **6** are much smaller than the redox potential shift induced by the different substituents (MeO, Me) attached to the triphenylamine units. The fact that there is a larger gap (approximately 120–150 mV) between the redox potentials of $\mathbf{M}^{2+}/\mathbf{M}^{3+}$ and $\mathbf{M}^{3+}/\mathbf{M}^{4+}$ for **5** and **6** allows the selective generation of the $\mathbf{M}^{3+}$ triradical trication. The trications $\mathbf{5}^{3+}$ and $\mathbf{6}^{3+}$ will be the focus of the following sections.

Spectroelectrochemistry: The radical cations of **5** and **6** were investigated by UV/Vis/NIR spectroscopy using a spectroelectrochemical set-up described elsewhere.[61] With this device, UV/Vis/NIR spectra can be measured, while the compound under investigation is oxidised or reduced step-by-step by applying an electrical potential to an optically transparent gold minigrid working electrode, which is squeezed between two quartz windows. The solution layer (100 μm) between these quartz plates was completely electrolysed at each potential applied, and the UV/Vis/NIR spectra were recorded in transmission.

Upon oxidation, both compounds **5** and **6** showed a broad band in the NIR spectra at approximately 7000–7500 cm^{-1} (Figure 2). We assigned this band to an intervalence charge-transfer (IV-CT) excitation of the radical cations $\mathbf{M}^{+}$–$\mathbf{M}^{5+}$. The band intensity is maximal for $\mathbf{M}^{3+}$, which can be selectively generated owing to the large potential gap between $\mathbf{M}^{3+}$ and $\mathbf{M}^{4+}$. This IV-CT band disappears when $\mathbf{M}^{3+}$ is further oxidised to $\mathbf{M}^{6+}$. In addition, there is a very intense band at around 13400 cm^{-1} which we assigned to a π–π^* band of the localised triarylamine radical cation.[62–64] This radical band is maximal for $\mathbf{M}^{6+}$. In general, the spectra for $\mathbf{5}^{n+}$

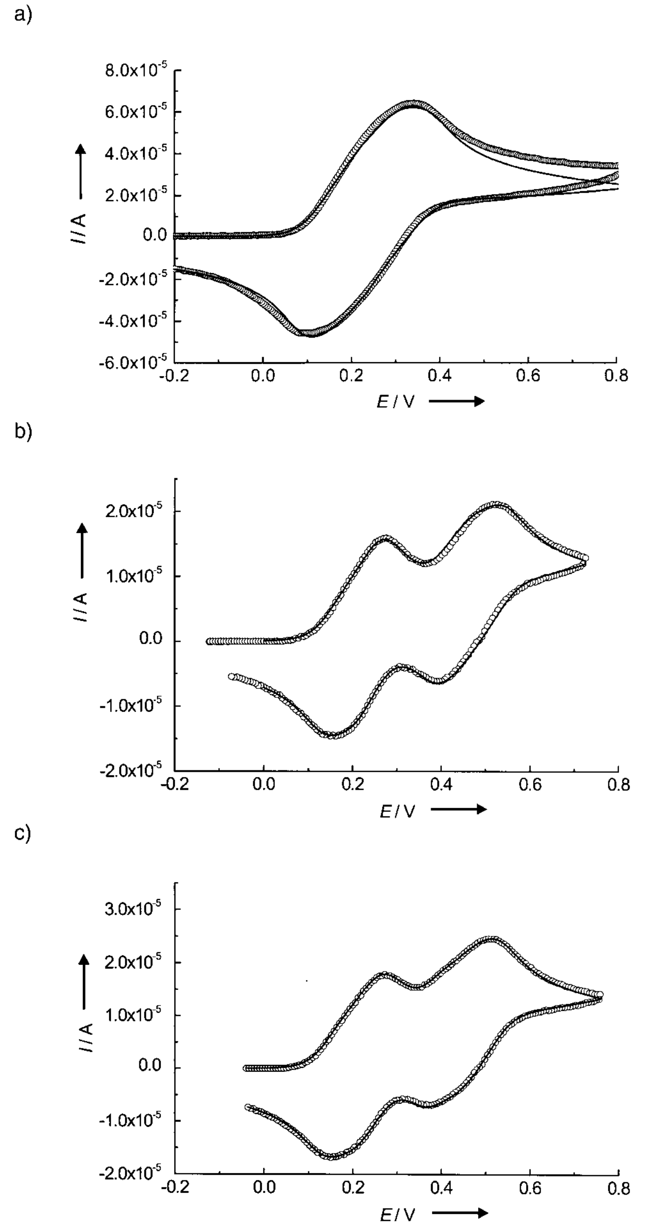

Figure 1. Cyclic voltammetry of a) **3**, b) **5** and c) **6** in 0.1M TBAH versus Fc/Fc$^+$ in CH_2Cl_2 at 250 mV s^{-1}. Experimental values: open circles. Simulated values: solid lines.

Table 1. Redox potentials of **3**, **5** and **6** determined by cyclic voltammetry in CH_2Cl_2/0.1M TBAHF versus Fc/Fc$^+$.

	$E^o_{1/2}(\mathbf{2}^{n+}/\mathbf{2}^{n+1+})$ [mV][a]	$E^o_{1/2}(\mathbf{5}^{n+}/\mathbf{5}^{n+1+})$ [mV][a]	$E^o_{1/2}(\mathbf{6}^{n+}/\mathbf{6}^{n+1+})$ [mV][a]
M/M$^+$	133	159	155
M$^+$/M^{2+}	176	216	215
M^{2+}/M^{3+}	214	256	260
M^{3+}/M^{4+}	252	404	382
M^{4+}/M^{5+}	287	456	448
M^{5+}/M^{6+}	314	516	505

[a] ±2 mV.

and $\mathbf{6}^{n+}$ do not differ greatly in their shape, but mainly in the intensity of the IV-CT band of $\mathbf{5}^{3+}$ ($\varepsilon = 5140\,\text{M}^{-1}\text{cm}^{-1}$) and $\mathbf{6}^{3+}$ ($\varepsilon = 2940\,\text{M}^{-1}\text{cm}^{-1}$). In Figure 2, the IVCT bands of $\mathbf{5}^{3+}$ and $\mathbf{6}^{3+}$ are given together with their deconvolution by fitting with Gaussian curves, which is assumed to be the proper band shape for IV-CT bands with a width at half-maximum at the high-temperature limit of $\tilde{\nu}_{1/2}(\text{HTL}) = 47.94\sqrt{\lambda}$ where λ is the Marcus reorganisation energy.[29] The optical data of the IV-CT bands are given in Table 2. The observed bandwidths are distinctly broader than the theoretical HTL value. This is often observed, but in our case this may be a result of the overlap of different bands at slightly different energies (see below).

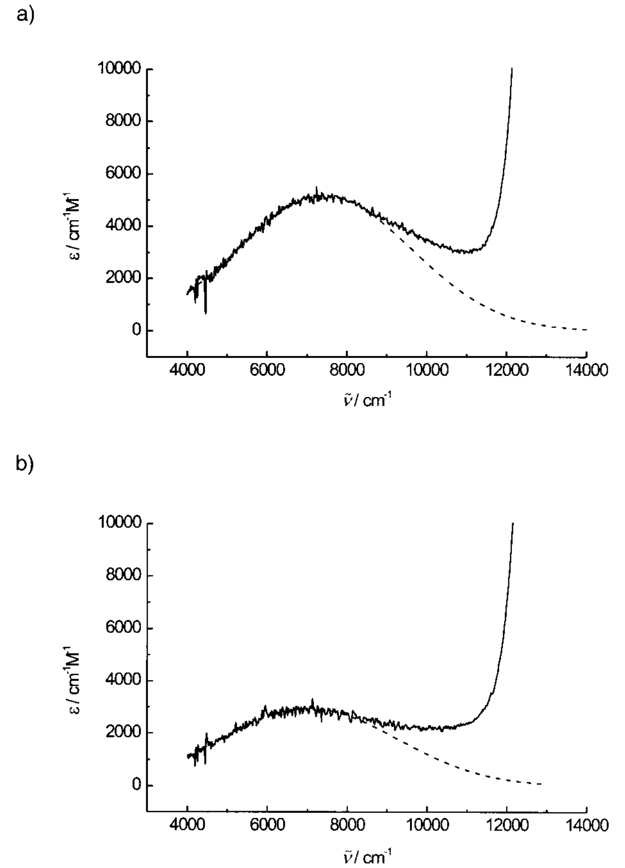

Figure 2. UV/Vis/NIR spectra of a) $\mathbf{5}^{3+}$ and b) $\mathbf{6}^{3+}$ in CH_2Cl_2/0.1M TBAH measured in a spectoelectrochemical thin-layer cell. Gaussian fit as dashed line.

Table 2. Optical properties of the IV-CT band of $\mathbf{5}^{3+}$ and $\mathbf{6}^{3+}$.

	$\tilde{\nu}_{max}$ [cm^{-1}][a]	λ [cm^{-1}]	$\tilde{\nu}_{1/2}$ [cm^{-1}][b]	$\tilde{\nu}_{1/2}$(HTL) [cm^{-1}]	ε [M^{-1}cm^{-1}][c]	μ_{eg} [D][d]	$\Delta\mu_{ab}$ [D]	V [cm^{-1}][e]
$\mathbf{5}^{3+}$	7450	7050[f]	5100	4020	5140	5.9	34.1	530
$\mathbf{6}^{3+}$	7040	6960[g]	5200	4000	2940	4.6	34.1	480

[a] ±50 cm^{-1}. [b] ±100 cm^{-1}. [c] ±300 M^{-1} cm^{-1}. [d] ±0.2 D. [e] ±20 cm^{-1}. [f] Calculated with $\lambda = \tilde{\nu}_{max}(\mathbf{5}^{3+}) - R - \Delta G^0$. [g] Calculated with $\lambda = \tilde{\nu}_{max}(\mathbf{6}^{3+}) + R - \Delta G^0$.

Theoretical analysis of the excited states: By applying a similar methodology to that used with **1**,[40] we will describe the electronic coupling within the radical trications of **5** and **6** and analyse the experimental IV-CT bands accordingly. We will first describe in detail the theoretical analysis for $\mathbf{5}^{3+}$; we will then only give the results for $\mathbf{6}^{3+}$, as its analysis is analogous.

0947-6539/02/0815-3470 $ 20.00+.50/0

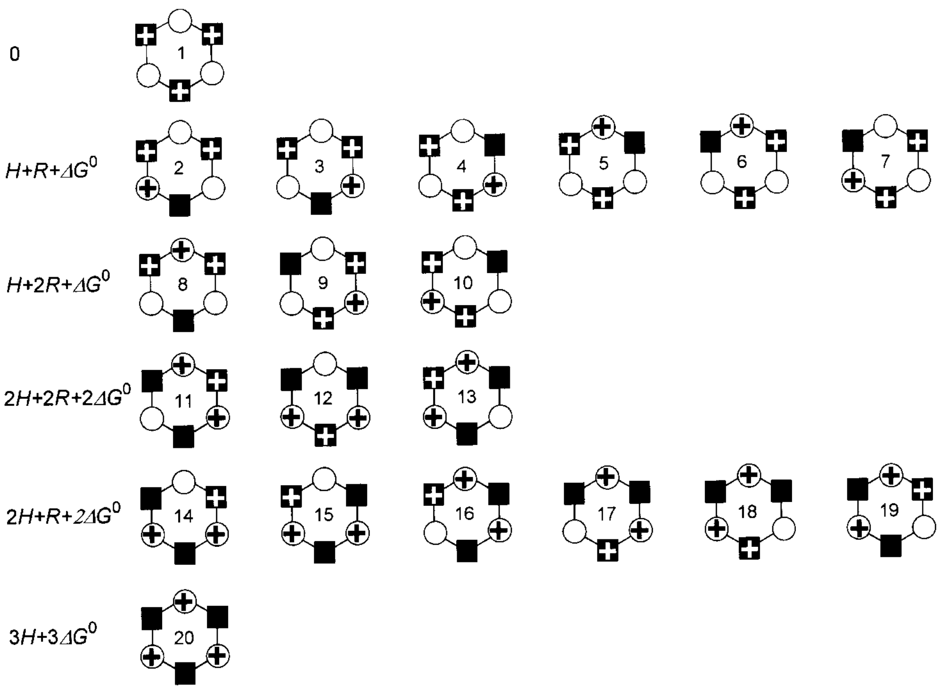

Scheme 3. All diabatic states of $\mathbf{5}^{3+}$ and their corresponding diabatic site energies.

The set of diabatic (noninteracting) states, which were coupled by the multi-dimensional Mulliken–Hush formalism, is given in Scheme 3. Because we will first deal with Franck–Condon excitations, the geometry of all these states is that of the lowest energy diabatic state 1. In the states of Scheme 3, ⊞ assigns a methoxy-substituted triarylamine radical cation in its relaxed geometry, ○ is a neutral methyl-substituted triarylamine in its relaxed geometry, ■ represents a neutral methoxy-substituted triarylamine centre in the geometry of a radical cation triarylamine and ⊕ is a methyl-substituted triarylamine radical cation in the geometry of a neutral triarylamine. While the diabatic state 1 is lowest in energy (all radical cation centres adopt the geometry of a triarylamine radical cation), the states 2–7 have the state energy $H+R+\Delta G^0$ (one radical cation centre is in the neutral geometry and one neutral centre is in the radical cation geometry) where H is the diabatic potential, R is an electrostatic repulsion which arises because of two cationic centres being in the *ortho* position, and ΔG^0 is due to the different local redox potentials of methyl- and methoxy-substituted triarylamines. The states 8–10 only differ from 2–7 in an additional repulsion R: $H+2R+\Delta G^0$. The states 11–13 and 14–19 have the relative energy $2H+2R+2\Delta G^0$ and $2H+R+2\Delta G^0$, respectively (two radical cation centres are in the neutral geometry and two neutral centres are in the radical cation geometry). Finally, state 20 is at energy $3H+3\Delta G^0$ (all radical centres are in the neutral geometry and all neutral centres are in the radical cation geometry). These 20 diabatic states of Scheme 3 can be coupled in a 20 × 20 secular determinant [Eq. (4)].

$$\left|\begin{array}{ccccccc|ccccccccccccc}
-\varepsilon & V_{\mathrm{o}} & V_{\mathrm{o}} & V_{\mathrm{o}} & V_{\mathrm{o}} & V_{\mathrm{o}} & V_{\mathrm{o}} & V_{\mathrm{p}} & V_{\mathrm{p}} & V_{\mathrm{p}} & 0 & 0 & 0 & 0 & 0 & 0 & 0 & 0 & 0 & 0 \\
V_{\mathrm{o}} & H+R+\Delta G^0-\varepsilon & V_{\mathrm{m}} & 0 & 0 & 0 & V_{\mathrm{m}} & V_{\mathrm{m}} & 0 & V_{\mathrm{m}} & 0 & 0 & V_{\mathrm{o}} & V_{\mathrm{p}} & V_{\mathrm{o}} & 0 & 0 & 0 & V_{\mathrm{o}} & 0 \\
V_{\mathrm{o}} & V_{\mathrm{m}} & H+R+\Delta G^0-\varepsilon & V_{\mathrm{m}} & 0 & 0 & 0 & V_{\mathrm{m}} & V_{\mathrm{m}} & 0 & V_{\mathrm{o}} & 0 & 0 & V_{\mathrm{o}} & V_{\mathrm{p}} & V_{\mathrm{o}} & 0 & 0 & 0 & 0 \\
V_{\mathrm{o}} & 0 & V_{\mathrm{m}} & H+R+\Delta G^0-\varepsilon & V_{\mathrm{m}} & 0 & 0 & 0 & V_{\mathrm{m}} & V_{\mathrm{m}} & 0 & V_{\mathrm{o}} & 0 & 0 & V_{\mathrm{o}} & V_{\mathrm{p}} & V_{\mathrm{o}} & 0 & 0 & 0 \\
V_{\mathrm{o}} & 0 & 0 & V_{\mathrm{m}} & H+R+\Delta G^0-\varepsilon & V_{\mathrm{m}} & 0 & V_{\mathrm{m}} & 0 & V_{\mathrm{m}} & 0 & 0 & V_{\mathrm{o}} & 0 & 0 & V_{\mathrm{o}} & V_{\mathrm{p}} & V_{\mathrm{o}} & 0 & 0 \\
V_{\mathrm{o}} & 0 & 0 & 0 & V_{\mathrm{m}} & H+R+\Delta G^0-\varepsilon & V_{\mathrm{m}} & V_{\mathrm{m}} & V_{\mathrm{m}} & 0 & V_{\mathrm{o}} & 0 & 0 & 0 & 0 & 0 & V_{\mathrm{o}} & V_{\mathrm{p}} & V_{\mathrm{o}} & 0 \\
V_{\mathrm{o}} & V_{\mathrm{m}} & 0 & 0 & 0 & V_{\mathrm{m}} & H+R+\Delta G^0-\varepsilon & 0 & V_{\mathrm{m}} & V_{\mathrm{m}} & 0 & V_{\mathrm{o}} & 0 & V_{\mathrm{o}} & 0 & 0 & 0 & V_{\mathrm{o}} & V_{\mathrm{p}} & 0 \\
\hline
V_{\mathrm{p}} & V_{\mathrm{m}} & V_{\mathrm{m}} & 0 & V_{\mathrm{m}} & V_{\mathrm{m}} & & H+2R+\Delta G^0-\varepsilon & 0 & 0 & V_{\mathrm{p}} & 0 & V_{\mathrm{p}} & 0 & 0 & V_{\mathrm{o}} & 0 & 0 & V_{\mathrm{o}} & 0 \\
V_{\mathrm{p}} & 0 & V_{\mathrm{m}} & V_{\mathrm{m}} & 0 & V_{\mathrm{m}} & V_{\mathrm{m}} & 0 & H+2R+\Delta G^0-\varepsilon & 0 & V_{\mathrm{p}} & V_{\mathrm{p}} & 0 & V_{\mathrm{o}} & 0 & 0 & V_{\mathrm{o}} & 0 & 0 & 0 \\
V_{\mathrm{p}} & V_{\mathrm{m}} & 0 & V_{\mathrm{m}} & V_{\mathrm{m}} & 0 & V_{\mathrm{m}} & 0 & 0 & H+2R+\Delta G^0-\varepsilon & 0 & V_{\mathrm{p}} & V_{\mathrm{p}} & 0 & V_{\mathrm{o}} & 0 & 0 & V_{\mathrm{o}} & 0 & 0 \\
0 & 0 & V_{\mathrm{o}} & 0 & 0 & V_{\mathrm{o}} & 0 & V_{\mathrm{p}} & V_{\mathrm{p}} & 0 & 2H+2R+2\Delta G^0-\varepsilon & 0 & 0 & V_{\mathrm{m}} & 0 & V_{\mathrm{m}} & V_{\mathrm{m}} & 0 & V_{\mathrm{m}} & V_{\mathrm{p}} \\
0 & 0 & 0 & V_{\mathrm{o}} & 0 & 0 & V_{\mathrm{o}} & 0 & V_{\mathrm{p}} & V_{\mathrm{p}} & 0 & 2H+2R+2\Delta G^0-\varepsilon & 0 & V_{\mathrm{m}} & V_{\mathrm{m}} & 0 & V_{\mathrm{m}} & V_{\mathrm{m}} & 0 & V_{\mathrm{p}} \\
0 & V_{\mathrm{o}} & 0 & 0 & V_{\mathrm{o}} & 0 & 0 & V_{\mathrm{p}} & 0 & V_{\mathrm{p}} & 0 & 0 & 2H+2R+2\Delta G^0-\varepsilon & 0 & V_{\mathrm{m}} & V_{\mathrm{m}} & 0 & V_{\mathrm{m}} & V_{\mathrm{m}} & V_{\mathrm{p}} \\
0 & V_{\mathrm{p}} & V_{\mathrm{o}} & 0 & 0 & 0 & 0 & 0 & V_{\mathrm{o}} & 0 & V_{\mathrm{m}} & V_{\mathrm{m}} & 0 & 2H+R+2\Delta G^0-\varepsilon & V_{\mathrm{m}} & 0 & 0 & 0 & V_{\mathrm{m}} & V_{\mathrm{o}} \\
0 & V_{\mathrm{o}} & V_{\mathrm{p}} & V_{\mathrm{o}} & 0 & 0 & 0 & 0 & 0 & V_{\mathrm{o}} & 0 & V_{\mathrm{m}} & V_{\mathrm{m}} & V_{\mathrm{m}} & 2H+R+2\Delta G^0-\varepsilon & V_{\mathrm{m}} & 0 & 0 & 0 & V_{\mathrm{o}} \\
0 & 0 & V_{\mathrm{o}} & V_{\mathrm{p}} & V_{\mathrm{o}} & 0 & 0 & V_{\mathrm{o}} & 0 & 0 & V_{\mathrm{m}} & 0 & V_{\mathrm{m}} & 0 & V_{\mathrm{m}} & 2H+R+2\Delta G^0-\varepsilon & V_{\mathrm{m}} & 0 & 0 & V_{\mathrm{o}} \\
0 & 0 & 0 & V_{\mathrm{o}} & V_{\mathrm{p}} & V_{\mathrm{o}} & 0 & 0 & V_{\mathrm{o}} & 0 & V_{\mathrm{m}} & V_{\mathrm{m}} & 0 & 0 & 0 & V_{\mathrm{m}} & 2H+R+2\Delta G^0-\varepsilon & V_{\mathrm{m}} & 0 & V_{\mathrm{o}} \\
0 & 0 & 0 & 0 & V_{\mathrm{o}} & V_{\mathrm{p}} & V_{\mathrm{o}} & 0 & 0 & V_{\mathrm{o}} & 0 & V_{\mathrm{m}} & V_{\mathrm{m}} & 0 & 0 & 0 & V_{\mathrm{m}} & 2H+R+2\Delta G^0-\varepsilon & V_{\mathrm{m}} & V_{\mathrm{o}} \\
0 & V_{\mathrm{o}} & 0 & 0 & 0 & V_{\mathrm{o}} & V_{\mathrm{p}} & V_{\mathrm{o}} & 0 & 0 & V_{\mathrm{m}} & 0 & V_{\mathrm{m}} & V_{\mathrm{m}} & 0 & 0 & 0 & V_{\mathrm{m}} & 2H+R+2\Delta G^0-\varepsilon & V_{\mathrm{o}} \\
0 & 0 & 0 & 0 & 0 & 0 & 0 & 0 & 0 & 0 & V_{\mathrm{p}} & V_{\mathrm{p}} & V_{\mathrm{p}} & V_{\mathrm{o}} & V_{\mathrm{o}} & V_{\mathrm{o}} & V_{\mathrm{o}} & V_{\mathrm{o}} & V_{\mathrm{o}} & 2H+3\Delta G^0-\varepsilon
\end{array}\right| = 0 \qquad (4)$$

Three different coupling elements can be distinguished: V_o describes the coupling between states in which the hole is transferred between two adjacent triarylamine centres (*ortho* positions of the hexaarylbenzene), V_m is the coupling between two states in which triarylamines in the *meta* position exchange a hole and V_p refers to the coupling between states in which triarylamines in the *para* positions exchange their hole. Couplings between two states in which more than one hole is exchanged vanish because the coupling operator is a one-electron operator as directly follows from its definition, [Eq. (1)].

Because Equation (4) is too complicated to be solved analytically, we have to make some simplifications: 1) States at $2H$ and $3H$ are omitted because there is no direct coupling from the ground state into these states. (Forbidden) transitions into these states will only result in very weak IV-CT bands at much higher energy than the IV-CT band observed in the spectroelectrochemistry. 2) The *meta* coupling V_m is set to zero because we expect it to be much smaller than V_o and V_p owing to the *meta* conjugation path.[38] V_p also is set to zero because it is expected to be smaller than V_o owing to the larger effective ET pathway [see Eq. (1)] between the triarylamine centres. Having performed these simplifications, determinant 4 reduces to Equation (5) in which only the diabatic states 1–7 are coupled (the (omitted) matrix element indices refer to the numbering of states in Scheme 3).

$$\begin{vmatrix} -\varepsilon & V & V & V & V & V & V \\ V & H+R+\Delta G^0-\varepsilon & 0 & 0 & 0 & 0 & 0 \\ V & 0 & H+R+\Delta G^0-\varepsilon & 0 & 0 & 0 & 0 \\ V & 0 & 0 & H+R+\Delta G^0-\varepsilon & 0 & 0 & 0 \\ V & 0 & 0 & 0 & H+R+\Delta G^0-\varepsilon & 0 & 0 \\ V & 0 & 0 & 0 & 0 & H+R+\Delta G^0-\varepsilon & 0 \\ V & 0 & 0 & 0 & 0 & 0 & H+R+\Delta G^0-\varepsilon \end{vmatrix} = 0 \qquad (5)$$

In this determinant, V_o is replaced by the effective coupling integral V. The eigenstates of this determinant are $\varepsilon_1 = ½(H+R+\Delta G^0) - ½\sqrt{(H+R+\Delta G^0)^2 + 24V^2}$, $\varepsilon_2 = \varepsilon_3 = \varepsilon_4 = \varepsilon_5 = \varepsilon_6 = H+R+\Delta G^0$ and $\varepsilon_7 = ½(H+R+\Delta G^0) + ½\sqrt{(H+R+\Delta G^0)^2 + 24V^2}$.[65] The fivefold degeneracy of the eigenstates at $\varepsilon_2 - \varepsilon_6$ is due to V_m being set to zero. Because V is small relative to $H+R+\Delta G^0$, $\varepsilon_1 \approx 0$ and the six excited states $\varepsilon_2 - \varepsilon_7$ are approximately at the energy $H+R+\Delta G^0$ in which H refers to the Marcus reorganisation energy λ. Thus, for the determination of V from the IV-CT band using Equation (1), we have to divide this equation by a symmetry factor of $\sqrt{6}$ which is derived from the six (nearly) degenerate excited states.[37]

For the 1,2,4-substituted isomer $\mathbf{6}^{3+}$, the theoretical analysis is analogous. Therefore, only the relevant five diabatic states at energy 0 and $H-R+\Delta G^0$ are given in Scheme 4 as well as the reduced determinant Equation (6) in which the same simplification has been made as in the case of $\mathbf{5}^{3+}$.

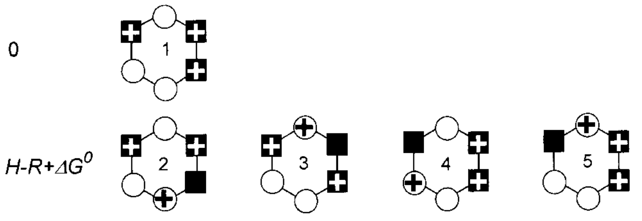

Scheme 4. A selection of diabatic states of $\mathbf{6}^{3+}$ and their corresponding diabatic site energies.

$$\begin{vmatrix} -\varepsilon & V & V & V & V \\ V & H-R+\Delta G^0-\varepsilon & 0 & 0 & 0 \\ V & 0 & H-R+\Delta G^0-\varepsilon & 0 & 0 \\ V & 0 & 0 & H-R+\Delta G^0-\varepsilon & 0 \\ V & 0 & 0 & 0 & H-R+\Delta G^0-\varepsilon \end{vmatrix} = 0 \qquad (6)$$

The eigenstates of this reduced determinant [Eq. (6)] are $\varepsilon_1 = ½(H-R+\Delta G^0) - ½\sqrt{(H-R+\Delta G^0)^2 + 16V^2}$, $\varepsilon_2 = \varepsilon_3 = \varepsilon_4 = H-R+\Delta G^0$ and $\varepsilon_5 = ½(H-R+\Delta G^0) + ½\sqrt{(H-R+\Delta G^0)^2 + 16V^2}$. Because V is small relative to $H-R+\Delta G^0$, $\varepsilon_1 \approx 0$ and the four excited states are approximately at the energy $H-R+\Delta G^0$. Again, for determining V from the IV-CT band by using Equation (1), we have to divide this equation by a symmetry factor of $\sqrt{4}$ which is derived from the four (nearly) degenerate excited states.[37] Because V is much smaller than $H/4$, we can directly estimate $R = 210\ \mathrm{cm}^{-1}$ from the difference of the IV-CT energies of $\mathbf{6}^{3+}$ and $\mathbf{5}^{3+}$ ($\tilde{\nu}_{\max}(\mathbf{5}^{3+}) - \tilde{\nu}_{\max}(\mathbf{6}^{3+}) \approx (H+R+\Delta G^0) - (H-R+\Delta G^0) = 2R$).

With Equation (1), the appropriate symmetry factors and the experimental optical data of the IV-CT bands (Table 2) we obtained $V = 530\ \mathrm{cm}^{-1}$ for $\mathbf{5}^{3+}$ and $V = 480\ \mathrm{cm}^{-1}$ for $\mathbf{6}^{3+}$. In Equation (1), $\Delta\mu_{ab}$ has been approximated by er in which r is the effective ET distance taken as the N–N distance (7.11 Å, from an AM1 calculation)[*]. The couplings calculated in this way agree within experimental error, which is reasonable as the *ortho* couplings in $\mathbf{5}^{3+}$ and $\mathbf{6}^{3+}$ should be approximately the same. This supports our simplifications made in the reduction to determinants 5 and 6, which assumes that $V \approx V_o$ and all other coupling elements are much smaller. The V values obtained for $\mathbf{5}^{3+}$ and $\mathbf{6}^{3+}$ are about 40 % of that of tolane $\mathbf{2}^{+}$ ($V = 1200\ \mathrm{cm}^{-1}$)[20] although the number of bonds between the nitrogen centres is the same in the tolane and in $\mathbf{5}^{3+}$ and $\mathbf{6}^{3+}$. These smaller couplings are due to the twisted aryl substituents (see AM1 computations below) in the hexaarylbenzene derivative, whereas the two phenyl rings in tolane $\mathbf{2}^{+}$ are coplanar.

---

[*] The effective ET distance in $\mathbf{5}^{3+}$ and $\mathbf{6}^{3+}$ was also estimated from an UHF-AM1 calculation: We used the AM1-computed structure of $\mathbf{8}^{3+}$ and replaced four adjacent diphenylamine groups by hydrogen atoms. This hexaphenylbenzene derivative $\mathbf{9}^{+}$ has only two triarylamine units in the *ortho* position. The adiabatic dipole moment of $\mathbf{9}^{+}$ was computed by an AM1-UHF calculation which gave 19.0 D. Therefore, the dipole moment difference amounts to 28.5 D, which was calculated as the vector difference of two 19.0 D dipole moment vectors oriented with an angle of 60°. The 28.5 D refer to an ET distance of 5.9 Å, which is somewhat smaller than the N–N distance. This is reasonable as the value was derived from adiabatic dipole moment difference. We stress that this short effective ET distance does not necessarily mean that the hole or electron is transferred through space rather than trough the central benzene ring.

Bonvoisin et al.[38] investigated systems in which triarylamine units are connected in the *meta* position to a benzene ring such as **7**. The radical cation $\mathbf{7}^+$ has an electronic coupling of 181 cm^{-1}. Because the phenyl substituents in $\mathbf{7}^+$ are presumably less twisted around the central benzene ring owing to smaller steric hindrance than in $\mathbf{5}^{3+}$, the *meta* coupling in our derivatives will be even smaller than 181 cm^{-1}. This strongly supports our assumption that the V_m value is much smaller than V_o (approximately 500 cm^{-1}) in our systems.

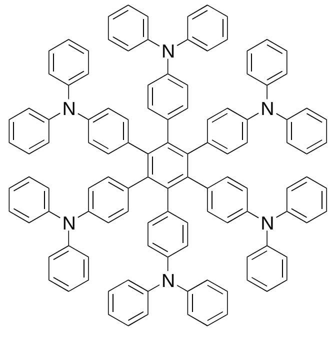

8

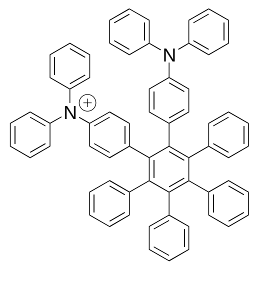

9⁺

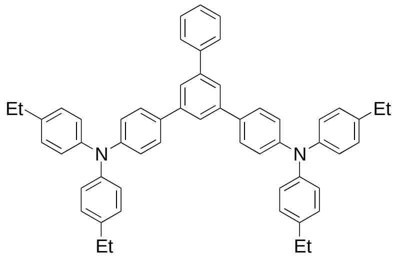

7

Semiempirical calculations: AM1 calculations[66] gave a reasonable estimate for the coupling integral in linear bis(triaryl)amine systems by using Koopman's theorem in which the ε(HOMO) – ε(HOMO – 1) energy difference of the neutral compound refers to $2V$.[20, 67] To estimate the coupling in the trimers $\mathbf{5}^{3+}$ and $\mathbf{6}^{3+}$, we used the D_6-symmetric derivative **8** without any methoxy or methyl groups and in which all six triarylamine centres are degenerate. Here, we have to use the six highest occupied orbitals from a RHF AM1 calculation (see Scheme 5). This orbital energy diagram was fitted by the solutions of the 6 × 6 secular determinant in Equation (7) which gave the best fit for $V_o = \pm 148$ cm^{-1}, $V_m = +64$ cm^{-1} and $V_p = \pm 49$ cm^{-1}. V_m is positive and V_o and V_p have opposite sign.

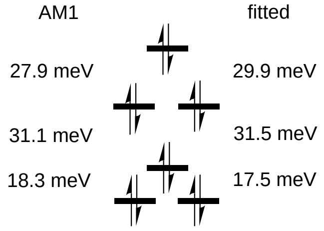

Scheme 5. AM1 calculated energy differences of the HOMOs of **8** and fitted differences using Equation (7).

$$\begin{vmatrix} -\varepsilon & V_o & V_m & V_p & V_p & V_o \\ V_o & -\varepsilon & V_o & V_m & V_p & V_p \\ V_m & V_o & -\varepsilon & V_o & V_m & V_p \\ V_p & V_m & V_o & -\varepsilon & V_o & V_m \\ V_p & V_p & V_m & V_o & -\varepsilon & V_o \\ V_o & V_p & V_p & V_m & V_o & -\varepsilon \end{vmatrix} = 0 \tag{7}$$

Although these couplings are distinctively smaller than those observed experimentally, it is apparent that the *ortho* coupling is the largest and dominates the coupling pattern. Thus, the fact that we completely neglected V_m and V_p in the previous analysis [Eqs. (5) and (6)] leads to V being an effective coupling integral. The underestimation of the computed couplings might be as a result of the twisting between the central benzene ring and the six adjacent phenyl substituents. The AM1-computed dihedral angle between these benzene rings might be too large, thus, diminishing the coupling.

We also performed CI calculations on the AM1-UHF-optimised geometry of $\mathbf{8}^{3+}$ (quartet state), which has D_3 symmetry.[68] In the UHF-optimised geometry the cationic (An$_2$N$^+$)benzene rings and the central benzene ring have a dihedral angle of 62.8°, whereas the neutral (An$_2$N)benzene ring has an angle of 82.8°. We used a full CI within an orbital window comprising of the three highest doubly occupied MOs and the three singly occupied MOs. The ground state was found to be a quartet state[69] followed by 19 excited quartet states and 70 doublet states (see Scheme 6). As excitations to the doublet states are forbidden by spin selection rules, we only consider the quartet states in the following discussion.

Two sets, each comprising nine excited quartet states, refer to single and double excitations, respectively, and one state refers to a triple excitation. The transition moments to the

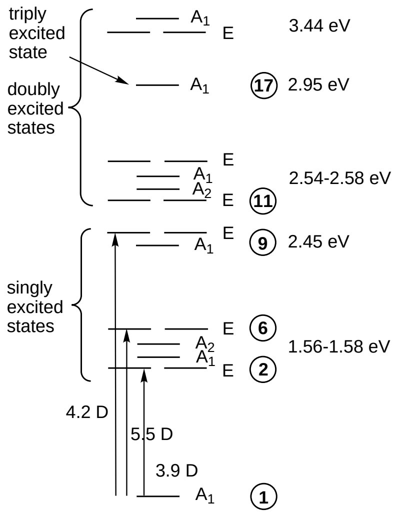

Scheme 6. State diagram of the AM1 CI calculation on $\mathbf{8}^{3+}$. The arrows indicate all excitations with significant transition moments. The splitting of the states is exaggerated compared to their relative energy position.

doubly and triply excited states vanish because the transition moment operator is a one-particle operator. Within the nine singly excited states, only transitions to the E states are significant: two allowed transitions were found into the E states out of a set of six singly-excited states quite close in energy (1.56 – 1.58 eV). These states refer to the six excited states of the solution of secular determinant 5, although their relative order is different. The transitions into the states at 1.56 – 1.58 eV are caused by the *ortho* couplings between the diabatic states 1 and 2 – 7. These two transitions are the IV-CT bands observed experimentally. As can be seen from the Coulson charge analysis of these states (2 and 6, Scheme 7), 3 × ⅓ e$^-$ are transferred by this excitation from the three neutral triarylamine centres in the ground state to the neighbouring positively charged triarylamine centres.

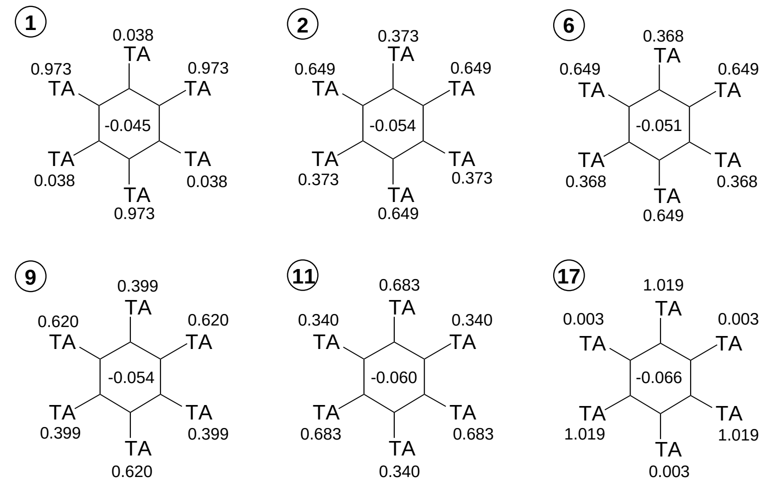

Scheme 7. AM1 CI calculated Coulson charges grouped together for the central benzene ring and the triarylamine moieties (TA) for the ground state (1) and the excited states (2, 6, 9, 11 and 17) of **8**$^{3+}$.

The third transition into a singly excited E state (9) is at much higher energy (2.45 eV) and is due to the *para* coupling between the diabatic states 1 and 8 – 10. Again, 3 × ⅓ e$^-$ are transferred by this excitation. The fact that the states at 2.45 eV are at considerably higher energy might be as a result of Coulombic repulsion in the diabatic states 8 – 10 which raise the energy compared to states 2 – 7. This repulsive energy is estimated from the experimental IV-CT energies to be approximately 2 × 210 cm^{-1} (see above) and might be exaggerated by the neglect of solvent influences in the AM1 computation.

As one can anticipate from its electronic origin, 3 × ⅔ e$^-$ are transferred in the doubly excited states, for example 11. In the triply excited state 17, 3 × 1 e$^-$ are transferred. In this state, the positively charged triarylamine centres change places with the neutral ones. This triply excited state refers to a concerted optically induced three-electron transfer, which is forbidden as a one-photon process.

In conclusion, our AM1-CI calculations suggest that the IV-CT band of **5**$^{3+}$ only consists of excitations caused by *ortho*-couplings and, consequently, V obtained from the IV-CT band analysis equals V_o with a good approximation.

Theoretical analysis of the ground state potential energy surface: Now, the question arises whether there is a thermally allowed concerted three-electron transfer in **5**$^{3+}$ in which all positively charged triarylamine centres change places with their neutral neighbours. To answer this question we coupled the states 1, 2, 4, 6, 15, 17, 19 and 20 (see Scheme 3) in the secular determinant [Eq. (8)] using quadratic potentials. These eight diabatic states were selected as they are connected by *ortho* couplings, which are by far the largest. The resulting adiabatic states (their character is very similar to the diabatic states in Scheme 3 (therefore, the numbering of states is analogous; however, the charged triarylamines are in their relaxed and neutral geometries) can be arranged in a "reaction cube" diagram (Scheme 8) in which the edges refer to one-dimensional ET processes between adjacent triarylamine moieties (*ortho* coupling). The three-dimensional concerted ET process refers to a path along the diagonal of the cube (see Scheme 8). An analogous diagram can be constructed using the adiabatic states 1, 3, 5, 7, 14, 16, 18 and 20.

The lowest energy solution of determinant 8 with $R = 210\,\mathrm{cm^{-1}}$, $\Delta G^0 = 290\,\mathrm{cm^{-1}}$, $V_o = 530\,\mathrm{cm^{-1}}$ and the reorganisation energy $\lambda = \tilde{\nu}_{\max} - R - \Delta G^0 = 7050\,\mathrm{cm^{-1}}$ is plotted depending on the ET coordinates x and $y = z$ in Figure 3. From this potential energy surface, it is obvious that the concerted three-electron transfer proceeds over a hilltop rather than over a true saddle point, that is this path is thermally forbidden. Instead, there are three consecutive one-electron

$$\begin{vmatrix}
\lambda(x^2+y^2+z^2) & V_o & V_o & V_o & 0 & 0 & 0 & 0 \\
V_o & \begin{matrix}\lambda((1-x)^2+y^2+z^2)\\+R+\Delta G^0\end{matrix} & 0 & 0 & V_o & 0 & V_o & 0 \\
V_o & 0 & \begin{matrix}\lambda(x^2+(1-y)^2+z^2)\\+R+\Delta G^0\end{matrix} & 0 & V_o & V_o & 0 & 0 \\
V_o & 0 & 0 & \begin{matrix}\lambda((x^2+y^2+(1-z)^2)\\+R+\Delta G^0\end{matrix} & 0 & V_o & V_o & 0 \\
0 & V_o & V_o & 0 & \begin{matrix}\lambda((1-x)^2+(1-y)^2+z^2)\\+R+2\Delta G^0\end{matrix} & 0 & 0 & V_o \\
0 & 0 & V_o & V_o & 0 & \begin{matrix}\lambda((x^2+(1-y)^2+(1-z)^2)\\+R+2\Delta G^0\end{matrix} & 0 & V_o \\
0 & V_o & 0 & V_o & 0 & 0 & \begin{matrix}\lambda((1-x)^2+y^2+(1-z)^2)\\+R+2\Delta G^0\end{matrix} & V_o \\
0 & 0 & 0 & 0 & V_o & V_o & V_o & \begin{matrix}\lambda((1-x)^2+(1-y)^2+(1-z)^2)\\+3\Delta G^0\end{matrix}
\end{vmatrix} = 0 \quad (8)$$

transfer steps that lead from the starting point (adiabatic state 1) to the adiabatic state 20. Whereas in Figure 3 the saddle point between state 1 and 2 is a true transition state, that between 2 and 20 is not because this is a (forbidden) two-dimensional two-electron transfer and there is a lower energy one-electron transfer pathway through state 19 (see also Scheme 8).

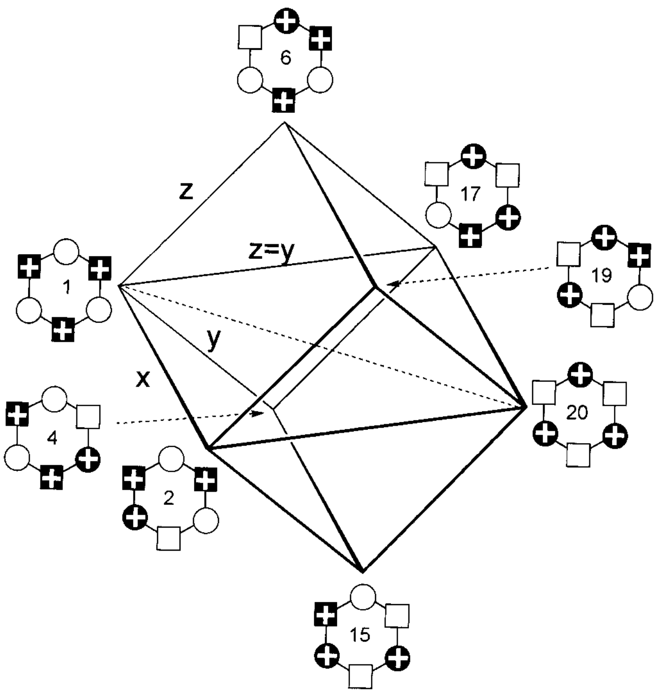

Scheme 8. Reaction diagram for the ET processes caused by *ortho*-couplings in 5^{3+}. The edges of the cube refer to one-electron transfer pathways between the indicated adiabatic states and the dashed line refers to a concerted three-electron transfer pathway.

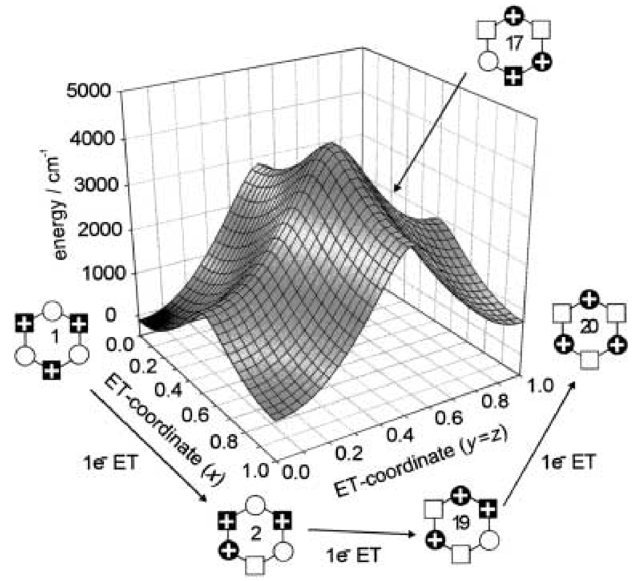

Figure 3. Ground state potential energy surface of 5^{3+} from the minimum energy solution of Equation (8). The ET coordinates refer to Scheme 8.

Conclusion

In this study we have investigated the optically and thermally induced electron transfer pathways of a highly symmetrical (D_3) hexaarylbenzene systems **5** with six triarylamine redox sites and its isomer **6**. Owing to slightly different local redox potentials, we were able to generate the trication $\mathbf{5}^{3+}$ selectively by electrochemical methods. This trication has a strong IV-CT band in the NIR that was subsequently analysed using multi-dimensional Mulliken–Hush theory. In combination with quantum chemical AM1 CI calculations, we were able to demonstrate that there is no optically induced concerted three-electron transfer that transforms the ground state into a state where all three positively charged triarylamine moieties change place with their neutral neighbours because this transfer is forbidden as a one-photon process. This corrects our earlier interpretation for the case of **8** in which we assumed two-dimensional ET processes because of the E and A symmetry of the excited CT states.[21]

We also constructed the potential energy surface of the ground state of $\mathbf{5}^{3+}$ by using quadratic potentials. From this potential surface it is apparent that there is also no thermally allowed concerted three-electron transfer pathway. Instead, three consecutive one-electron transfer steps are necessary for this process. The conclusions equally apply to $\mathbf{3}^{3+}$, which is derived from **3** and has an even higher symmetry (D_6). These fundamental findings might have implications for many symmetrical ET systems that can also be found in nature. For example, the photosynthetic reaction centres of both the purple bacteria *Rhodopseudomonas viridis*[70, 71] and that of the cyanobacteria *Synechococcus elongatus*[72] have pseudo-C_2 symmetry with two ET branches. It is currently our goal to elucidate which basic structural factors are necessary to promote concerted two-dimensional ET processes.

Experimental Section

1,3,5-Tris[*N*,*N*-di(4-methoxyphenyl)-4-aminophenyl]-2,4,6-tris[*N*,*N*-di-(4-methylphenyl)-4-aminophenyl]benzene (5) and 1,2,4-tris[*N*,*N*-di(4-methoxyphenyl)-4-aminophenyl]-3,5,6-tris[*N*,*N*-di(4-methylphenyl)-4-aminophenyl]benzene (6): Tolane **4** (100 mg, 0.17 mmol) was dissolved in dry methylcyclohexane (5 mL) under a nitrogen atmosphere and was heated to 60 °C. Dicobaltoctacarbonyl (12 mg, 0.04 mmol) was added, and the mixture was heated at reflux (ca. 101 °C) for 3 h. The solvent was evaporated, and the residue was purified by flash chromatography (solvent gradient petrol ether/CH_2Cl_2 2:1 → CH_2Cl_2 → CH_2Cl_2/MeOH 50:1). The products were dissolved in ethyl acetate and precipitated by dropping into an excess of petroleum ether to afford compounds **5** (20 mg, 20 % yield) and **6** (60 mg, 60 % yield) as colourless solids.

Compound 5: ^1H NMR (400 MHz, CD_2Cl_2, 25 °C): $\delta = 6.99$, 6.84 (AA′, BB′, 2 × 12 H; arom.), 6.89, 6.76 (AA′, BB′, 2 × 12 H; arom.), 6.72, 6.60 (AA′, BB′, 2 × 6 H; aminophenyl), 6.67 (AA′-BB′, 12 H; aminophenyl), 3.72 (s, 18 H; methoxy), 2.25 ppm (s, 18 H; methyl); ^{13}C NMR (100.6 MHz, CD_2Cl_2, 25 °C): $\delta = 155.7$, 146.3, 145.7, 145.9, 141.8, 140.6, 140.6, 135.9, 134.5, 132.8, 132.7, 132.1, 130.1, 126.0, 124.1, 122.6, 120.6, 114.9, 55.7 (C-9), 20.8 ppm.

Compound 6: ^1H NMR (400 MHz, CD_2Cl_2, 25 °C): $\delta = 6.99$, 6.84 (m, 3 × AA′, 3 × BB′, 24 H; arom.), 6.89, 6.76 (3 × AA′, 3 × BB′, 24 H; aroma.), 6.72, 6.60 (3 × AA′, 3 × BB′, 12 H; aminophenyl), 6.67 (3 × AA′-BB′, 12 H; aminophenyl), 3.72 (3 × s, 18 H; methoxy), 2.25 ppm (3 × s, 18 H; methyl); ^{13}C NMR (100.6 MHz, CD_2Cl_2, 25 °C): $\delta = 155.8$, 155.8, 146.3, 146.3, 145.7, 145.7, 145.9, 141.8, 141.8, 140.6, 140.6, 140.6, 140.6, 140.6, 140.6, 135.9, 135.8, 135.8, 134.6, 134.6, 134.5, 132.8, 132.8, 132.7, 132.7, 132.1, 132.1, 130.1, 130.1, 126.0, 126.0, 124.1, 124.1, 122.6, 122.5, 120.7, 120.6, 114.9, 55.7, 20.8 ppm; HRMS (FAB, PI, mixture of both isomers): m/z calcd for $C_{126}H_{108}N_6O_6$ (1802.28): calcd 1800.8330; found: 1800.8247.

Cyclic voltammetry and spectroelectrochemistry: The electrochemical experiments were performed in dry, nitrogen-saturated CH_2Cl_2 with 0.1 M tetrabutylammonium hexafluorophosphate (TBAH) as supporting electrolyte and 0.001 M substrate. The potentials were referenced against ferrocene (Fc/Fc$^+$). Digital fits of the experimental cyclic voltammograms were done with DigiSim[60] with the assumption of chemical and electrochemical reversibility of all processes. For spectroelectrochemical analysis, the solution of the CV experiments was transferred into a thin-layer cell[61] that comprised two quartz windows in between which was squeezed a gold minigrid working electrode. The optical path length was 100 μm. The cell design has been described elsewhere.[61] The UV/Vis/NIR spectra were recorded with a Perkin–Elmer lambda-9 spectrometer in transmission mode.

Semiempirical calculations: Using the AM1 hamiltonian implemented in the MOPAC97 program package,[66] we optimised the structure of **8** in D_6 symmetry. This high symmetry was imposed because triarylamines are known to have a planar coordinate nitrogen,[73] while AM1 predicts a pyramidalised nitrogen that would lead to symmetry lowering (C_3) for **8**. The trication $\mathbf{8}^{3+}$ was optimised at the UHF level as a quartet state within D_3 symmetry. Based on this geometry we performed a CI calculation with an active orbital window comprising the three highest doubly and the three highest singly occupied orbitals. This CI corresponds to a CISDT. The CI calculation gave a quartet ground state followed by a set of degenerate doublet states only 0.0008 eV higher in energy. Thus, one can expect $\mathbf{8}^{3+}$ to be a mixture of quartet and doublet states even at low temperature. For each excited quartet state there is a set of two excited doublet states very close in energy. However, the discussion of excited state properties is restricted to the quartet states only.

Acknowledgement

This work was supported by the Fonds der Chemischen Industrie and the Deutsche Forschungsgemeinschaft. We thank Prof. J. Daub for his kind support during the work in Regensburg.

---

[1] P. F. Barbara, T. J. Meyer, M. A. Ratner, *J. Phys. Chem.* **1996**, *100*, 13148.
[2] *Chem. Rev.* **1992**, *92*, 369. This issue is devoted to ET processes in biologically relevant systems.
[3] C. Creutz, *Progr. Inorg. Chem.* **1983**, *30*, 1.
[4] D. E. Richardson, H. Taube, *Coord. Chem. Rev.* **1984**, *60*, 107.
[5] K. D. Demadis, C. M. Hartshorn, T. J. Meyer, *Chem. Rev.* **2001**, *101*, 2655.
[6] S. Mazur, C. Streekumar, A. H. Schroeder, *J. Am. Chem. Soc.* **1976**, *98*, 6713.
[7] A. H. Schroeder, S. Mazur, *J. Am. Chem. Soc.* **1978**, *100*, 7339.
[8] T. H. Jozefiak, J. E. Almlof, M. W. Feyereisen, L. L. Miller, *J. Am. Chem. Soc.* **1989**, *111*, 4105.
[9] S. F. Rak, L. L. Miller, *J. Am. Chem. Soc.* **1992**, *114*, 1388.
[10] S. F. Nelsen, H. Chang, J. J. Wolff, J. Adamus, *J. Am. Chem. Soc.* **1993**, *115*, 12276.
[11] J. Bonvoisin, J.-P. Launay, C. Rovira, J. Veciana, *Angew. Chem.* **1994**, *106*, 2190; *Angew. Chem. Int. Ed.* **1994**, *33*, 2106.
[12] K. Lahlil, A. Moradpour, C. Bowlas, F. Menou, P. Cassoux, J. Bonvoisin, J.-P. Launay, G. Dive, D. Dehareng, *J. Am. Chem. Soc.* **1995**, *117*, 9995.
[13] S. F. Nelsen, D. A. Trieber II, J. J. Wolff, D. R. Powell, S. Rogers-Crowley, *J. Am. Chem. Soc.* **1997**, *119*, 6873.
[14] S. F. Nelsen, R. F. Ismagilov, D. R. Powell, *J. Am. Chem. Soc.* **1997**, *119*, 10213.
[15] S. F. Nelsen, R. F. Ismagilov, D. A. Trieber II, *Science* **1997**, *278*, 846.
[16] S. F. Nelsen, M. T. Ramm, J. J. Wolff, D. R. Powell, *J. Am. Chem. Soc.* **1997**, *119*, 6863.
[17] S. F. Nelsen, R. F. Ismagilov, D. R. Powell, *J. Am. Chem. Soc.* **1998**, *120*, 1924.
[18] S. F. Nelsen, R. F. Ismagilov, Y. Teki, *J. Am. Chem. Soc.* **1998**, *120*, 2200.
[19] S. F. Nelsen, H. Q. Tran, R. F. Ismagilov, M. T. Ramm, L.-J. Chen, D. R. Powell, *J. Org. Chem.* **1998**, *63*.
[20] C. Lambert, G. Nöll, *J. Am. Chem. Soc.* **1999**, *121*, 8434.
[21] C. Lambert, G. Nöll, *Angew. Chem.* **1998**, *110*, 2239; *Angew. Chem. Int. Ed.* **1998**, *37*, 2107.
[22] C. Rovira, D. Ruiz-Molina, O. Elsner, J. Vidal-Gancedo, J. Bonvoisin, J.-P. Launay, J. Veciana, *Chem. Eur. J.* **2001**, *7*, 240.
[23] R. Kosloff, M. A. Ratner, *Isr. J. Chem.* **1990**, *30*, 45.
[24] N. Sutin, *Progr. Inorg. Chem.* **1983**, *30*, 441.
[25] C. Creutz, M. D. Newton, N. Sutin, *J. Photochem. Photobiol. A* **1994**, *82*, 47.
[26] R. J. Cave, N. M. D, *Chem. Phys. Lett.* **1996**, *249*, 15.
[27] D. V. Matyushov, B. M. Ladanyi, *J. Phys. Chem. A* **1998**, *102*, 5027.
[28] M. D. Newton, *Adv. Chem. Phys.* **1999**, *106*, 303.
[29] N. S. Hush, *Coord. Chem. Rev.* **1985**, *64*, 135.
[30] a) E. Grunwald, *J. Am. Chem. Soc.* **1985**, *107*, 125; b) J. P. Guthrie, *J. Am. Chem. Soc.* **1996**, *118*, 12878.
[31] a) E. L. Bominaar, S. A. Borshch, J.-J. Girerd, *J. Am. Chem. Soc.* **1994**, *116*, 5362; b) A. J. Marks, K. Prassides, *J. Chem. Phys.* **1993**, *98*, 4805.
[32] T. Bandyopadhyay, A. Okada, M. Tachiya, *J. Chem. Phys.* **1999**, *110*, 9630.
[33] T. Motylewski, J. Najbar, M. Tachiya, *Chem. Phys.* **1996**, *212*, 193.
[34] J. Najbar, M. Tachiya, *J. Phys. Chem.* **1994**, *98*, 199.
[35] M.-a. Haga, M. M. Ali, H. Sato, H. Monjushiro, K. Nozaki, K. Kano, *Inorg. Chem.* **1998**, *37*, 2320.
[36] K. Aoki, J. Chen, M. Haga, *J. Electroanal. Chem.* **1995**, *396*, 309.
[37] a) J. Bonvoisin, J.-P. Launay, M. Van der Auweraer, F. C. De Schryver, *J. Phys. Chem.* **1994**, *98*, 5052; b) J. Bonvoisin, J.-P. Launay, W. Verbouwe, M. Van der Auweraer, F. C. De Schryver, *J. Phys. Chem.* **1996**, *100*, 17079.
[38] R. D. Cannon, L. Montri, D. B. Brown, K. M. Marshall, C. M. Elliott, *J. Am. Chem. Soc.* **1984**, *106*, 2591.
[39] C. Lambert, W. Gaschler, E. Schmälzlin, K. Meerholz, C. Bräuchle, *J. Chem. Soc. Perkin Trans. 2* **1999**, 577.
[40] C. Lambert, G. Nöll, F. Hampel, *J. Phys. Chem. A* **2001**, *105*, 7751.
[41] M. D. Watson, A. Fechtenkoetter, K. Muellen, *Chem. Rev.* **2001**, *101*, 1267.
[42] M. Müller, C. Kübel, K. Müllen, *Chem. Eur. J.* **1998**, *4*, 2099.
[43] R. Rathore, C. L. Burns, M. I. Deselnicu, *Org. Lett.* **2001**, *3*, 2887.
[44] J. Shi, C. H. Chen, S. A. Van Slyke, C. W. Tang, **1996**, *Vol. US-A 5554450*.
[45] M. M. Wienk, R. A. Janssen, *J. Am. Chem. Soc.* **1997**, *119*, 4492.
[46] M. Thelakkat, H. W. Schmidt, *Adv. Mater.* **1998**, *10*, 219.
[47] S. Sasaki, M. Iyoda, *Chem. Lett.* **1995**, *11*, 1011.
[48] K. Okada, T. Imakura, M. Oda, A. Kajiwara, M. Kamachi, K. Sato, D. Shiomi, T. Takui, K. Itoh, L. Gherghel, M. Baumgarten, *J. Chem. Soc. Perkin Trans. 2* **1997**, 1059.
[49] K. Yoshizawa, A. Chano, A. Ito, K. Tanaka, T. Yamabe, H. Fujita, J. Yamauchi, M. Shiro, *J. Am. Chem. Soc.* **1992**, *114*, 5994.
[50] A. Higuchi, H. Inada, T. Kobata, Y. Shirota, *Adv. Mater.* **1991**, *3*, 549.
[51] K. Katsuma, Y. Shirota, *Adv. Mater.* **1998**, *10*, 223.
[52] J. Louie, J. F. Hartwig, A. J. Fry, *J. Am. Chem. Soc.* **1997**, *119*, 11695.
[53] K. R. Stickley, S. C. Blackstock, *J. Am. Chem. Soc.* **1994**, *116*, 11576.
[54] K. R. Stickley, S. C. Blackstock, *Tetrahedron Lett.* **1995**, *36*, 1585.
[55] C. H. Chen, J. Shi, C. W. Tang, *Macromol. Symp.* **1997**, *125*, 1.
[56] I.-Y. Wu, J. T. Lin, Y.-T. Tao, E. Balasubramaniam, *Adv. Mater.* **2000**, *12*, 668.
[57] B. Speiser, M. Wurde, C. Maichle-Mossmer, *Chem. Eur. J.* **1998**, *4*, 222.
[58] K. P. C. Vollhardt, *Acc. Chem. Res.* **1977**, *10*, 1.
[59] C. Lambert, G. Nöll, unpublished results.
[60] M. Rudolph, S. W. Feldberg, DigiSim 3.03a, Bioanalytical Systems, Inc., West Lafayette, IN, USA, **1994–2000**.
[61] J. Salbeck, *Anal. Chem.* **1993**, *65*, 2169.
[62] S. Dapperheld, E. Steckhan, K.-H. G. Brinkhaus, T. Esch, *Chem. Ber.* **1991**, *124*, 2557.
[63] F. A. Neugebauer, S. Bamberger, W. R. Groh, *Chem. Ber.* **1975**, *108*, 2406.
[64] W. Schmidt, E. Steckhan, *Chem. Ber.* **1980**, *113*, 577.
[65] Maple V, Release 5, Waterloo Maple Inc., **1981–1997**.
[66] J. J. P. Stewart, MOPAC97, Fujitsu Limited, **1997**.

[67] M. N. Paddon-Row in *Electron Transfer in Chemistry, Vol. 3* (Ed.: V. Balzani), Wiley-VCH, Weinheim, **2001**, pp. 179.

[68] The AM1 calculations refer to the gas-phase. In solution, solvent-induced symmetry breaking might occur that leads to asymmetric charge distribution in the excited states, see J. J. Piet, W. Schuddeboom, B. R. Wegewijs, F. C. Groze, J. M. Warman, *J. Am. Chem. Soc.* **2001**, *123*, 5337 and W. Verbouwe, M. Van der Auweraer, F. C. D. Schryver, J. J. Piet, J. M. Warman, *J. Am. Chem. Soc.* **1998**, *120*, 1319. However, this phenomenon has no consequences for the present discussion of optically induced ET because we deal with Frank–Condon states and not with relaxed and possibly asymmetric excited states.

[69] The trication of **3**, **5**, **6** and **8** are expected to have high-spin (quartet) ground states, see, for example, ref. [48, 49].

[70] J. Deisenhofer, H. Michel, *Angew. Chem.* **1989**, *101*, 872; *Angew. Chem. Int. Ed.* **1989**, *28*, 829.

[71] R. Huber, *Angew. Chem.* **1989**, *101*, 849; *Angew. Chem. Int. Ed.* **1989**, *28*, 848.

[72] P. Jordan, P. Fromme, H. T. Witt, O. Klukas, W. Saenger, N. Krauss, *Nature* **2001**, *411*, 909.

[73] A. N. Sobolev, V. K. Bel'skii, I. P. Romm, N. Y. Chernikova, E. N. Guryanova, *Acta Crystallogr. Sect. C* **1985**, *C41*, 967.

Received: December 18, 2001
Revised: April 12, 2002 [F3746]